

1  
2  
3  
4  
5  
6  
7  
8  
9  
10  
11  
12  
13  
14  
15  
16  
17  
18  
19  
20  
21

---

# Water desorption characteristics of saturated lightweight fine aggregate in ultra-high performance concrete

Peiliang Shen<sup>1,2</sup>, Linnu Lu<sup>1,b</sup>, Fazhou Wang<sup>1,a</sup>, Yongjia He<sup>1</sup>, Shuguang Hu<sup>1</sup>,  
Jianxin Lu<sup>2</sup>, Haibing Zheng<sup>2</sup>

(<sup>1</sup> State Key Laboratory of Silicate Materials for Architectures, Wuhan  
University of Technology, Luoshi Road 122, Wuhan, 430070, China)

(<sup>2</sup>Department of Civil and Environmental Engineering, The Hong Kong  
Polytechnic University, Hung Hom, Kowloon, Hong Kong)

<sup>a</sup> Corresponding author, E-mail: fzhwang@whut.edu.cn;

<sup>b</sup> Corresponding author, E-mail: 383337652@qq.com;

---

1        **Abstract :** In this study, the water desorption behavior of saturated lightweight  
2 fine aggregate (LWA) in ultra-high performance concrete (UHPC) was systemmically  
3 investigated using isothermal calorimetry, relative humidity (RH), mercury intrusion  
4 porosimetry, X-ray microtomography methods, etc.. The LWA with high porosity and  
5 coarse pore structure exhibited high absorption and easy desorption at high RH. The  
6 results indicate that a large amount of water in LWA was released before setting,  
7 resulting in an increase of water to binder ratio, which had an adverse effect on the  
8 performance. However, the water absorbed in LWA released fast after 6 h, inducing an  
9 internal curing effect. Mechanism on a "four-stage desorption" driven by capillary  
10 pressure and RH gradient was proposed. The water desorption that is beneficial for the  
11 internal curing is calculated. The results indicated that the internal curing efficiency  
12 could be enhanced by increasing LWA content and reducing its pore size.

13        **Key words:** Ultra-high performance concrete; Water desorption; internal curing;  
14 relative humidity; lightweight fine aggregate;

15

---

# 1. Introduction

UHPC refers to a new type of advanced cement-based material exhibiting great mechanical properties and durability, which represents the highest development of high performance concrete [1-3]. However, the typical UHPC exhibits very high autogenous shrinkage due to low water to binder ratio, high content of superfine materials, absence of coarse aggregate and high content of cementitious materials [4-6]. Many methods have been applied to reduce the autogenous shrinkage, including the addition of expansive agents, coarse aggregate and internal curing materials [7-9]. Among these methods, introduction of internal curing materials such as super absorbent polymer (SAP), LWA and rice husk ash (RHA) can reduce the autogenous shrinkage effectively[10-12]. As the hydration products in bulk form occupy less space than water [13], the hydration reactions are accompanied by chemical shrinkage. The chemical shrinkage will produce physical shrinkage before setting and produce a self-desiccation due to the formation of partially-filled pores [14, 15]. The pore solution menisci remaining in partially filled pores will create a measurable capillary pressure, resulting in autogenous shrinkage. In the mixtures with lower water to binder ratios, this capillary pressure is higher due to the formation of vapor filled cavities in smaller radius of curvature [16]. The water desorption of saturated internal curing materials can provide additional readily-available source of water so that the capillary pores of matrix remains saturated, thus reducing the autogenous stresses and strains [10, 15]. The water desorption is a competition of water between internal curing materials and matrix. The

---

1 water in larger scale pores can be released into smaller pores motivated by relative  
2 humidity [17]. When the water in internal curing material is exhausted, the capillary stress  
3 and autogenous shrinkage will rapidly increase over time. Then, the water desorption of  
4 internal curing materials will affect the development of autogenous shrinkage,  
5 hydration and performance of concrete [18].

6 According the previous studies [11, 19], LWA is more effective in the reduction of  
7 shrinkage than other internal curing materials, as the water desorption of LWA is driven  
8 by capillary action. Therefore, the effects of saturated LWA on the performance of  
9 UHPC have been investigated. Some studies showed that the LWA had an adverse effect  
10 on the mechanical properties of UHPC [19, 20], while the enhancements of durability  
11 and mechanical properties by adding appropriate amount of LWA were also reported  
12 [19, 21]. These differences are certainly depended on the water absorption and  
13 desorption properties of LWA. The LWA has a complex behavior of water desorption  
14 under capillary action and RH gradient during hydration. This complex process is  
15 closely related to its effect on the performance of concrete. However, there is limited  
16 information on the water desorption of LWA in UHPC, and most of existing literature  
17 focus on that in the high performance concrete and ordinary concrete. The capillary  
18 pore structure and RH evolution of UHPC are rather different from those of ordinary  
19 concrete due to the large amount of superfine particles and low water to binder ratio  
20 [22, 23]. This will influence the process of water desorption of LWA and make it  
21 difficult to control the autogenous shrinkage. As a result, the water desorption process

---

1 of LWA in UHPC become a subject of great significance.

2 LWA is an artificial porous material, which is first produced in the 1930's for the  
3 production of lightweight blocks. It has been used in many applications such as  
4 masonry blocks, horticultural blends, filtration and civil engineering [24]. Also, The  
5 LWA has been used as an internal curing materials in high performance concrete due to  
6 its porous structure characteristic [25-28]. The results indicated that water desorption  
7 of LWA had significant effects on the internal curing effect, mechanical strength and  
8 pore structure evolution of concrete [27, 29, 30]. The primary hydration heat was moved  
9 up by adding LWA [10, 19]. In addition, the development of cumulative heat of  
10 hydration and degree of hydration were closely related to the water desorption of LWA.  
11 Several studies have investigated the desorption properties of LWA in concrete. For  
12 example, Landgren et al. investigated the absorption and desorption properties of coarse  
13 LWA used in US [31]. Bentz et al. determined the desorption isotherms by using salt  
14 solution to evaluate the water that was released into concrete due to self-desiccation  
15 [32], and found that most of the water within LWA was observed to be released during  
16 the first day's hydration [33]. Meanwhile, the water desorption from LWA exhibited a  
17 one-to-one agreement with measured chemical shrinkage. The time and distance of  
18 water movement from saturated LWA to cement paste were investigated by X-ray  
19 technique, which was important for mix design, shrinkage and stress development of  
20 concrete [34]. It should be noted that an internal curing affect zone around LWA was  
21 formed, as more water was consumed by this zone after setting [35]. Trtik et al. tested

---

1 water desorption of LWA using neutron radiography between 0.5 h and 20 h. It was found  
2 that the water desorption was a fast process, and the water was distributed homogeneously  
3 from the LWA to at least 3 mm into the paste [36]. In general, these literatures indicate  
4 that the water desorption process is of great significance for the working mechanism of  
5 LWA on the microstructure and performance of concrete.

6 The UHPC is different from normal concrete and high performance concrete,  
7 mainly reflects in its very low water to binder ratio and large amount of superfine  
8 particles, leading to a dense surrounding for LWA. This surrounding will influence the  
9 water desorption process of LWA, which leads to a different internal curing effect in  
10 UHPC compared to that of normal concrete. The previous studies showed that the LWA  
11 had an adverse effect on the performance of UHPC [19, 20], especially for UHPC with  
12 large amount of LWA. Generally, investigations on the effect of LWA on the  
13 performance of UHPC and the internal curing efficiency in UHPC are still very few,  
14 and the water desorption behavior of LWA in UHPC is also not clear.

15 The objective of this study is to investigate the water desorption characteristics of  
16 saturated LWA in UHPC and quantify the amount of water that releases during different  
17 curing ages. The water desorption behavior of LWA in UHPC was preliminarily  
18 characterized through measuring the internal RH development, hydration  
19 characteristics, workability and free water evolution. To obtain a deep understanding of  
20 the water desorption mechanism of saturated LWA in UHPC, the chemical shrinkage,  
21 autogenous shrinkage, X-ray microtomography images, pore structure and water

---

1 desorption of LWA under RH evolution of UHPC were measured. The water desorption  
2 process of LWA in UHPC was revealed on the basis of these measurements, and the  
3 amount of released water at different ages as well as the utilization rate of the internal  
4 curing water were quantified.

## 5 **2. Experiment**

### 6 **2.1 Materials**

7 Portland cement, silica fume and fly ash were used as cementitious materials.  
8 Their chemical compositions were listed in Table 1. LWA and quartz sand with the size  
9 between 0.15 mm and 1.18 mm were used as aggregates. The LWA was produced by  
10 expanded shale. The chemical composition of LWA was also listed in Table 1. The  
11 specific density of quartz sand is 2530kg/m<sup>3</sup>, and the wet specific density of LWA is  
12 1510kg/m<sup>3</sup>. The water absorption of LWA is 10.1%, which was tested after soaking in  
13 water for 24 h. Steel fiber (length=13mm, diameter=0.22mm) and superplasticizer were  
14 used as received. The dosage of steel fiber was 2% of the total volume of UHPC. The  
15 superplasticizer (produced by Sobute New Materials CO.,LTD) and tap water were also  
16 used.

17 Table 1 Chemical compositions of cementitious materials (wt. %)

Oxide	SiO <sub>2</sub>	Al <sub>2</sub> O <sub>3</sub>	CaO	Fe <sub>2</sub> O <sub>3</sub>	SO <sub>3</sub>	MgO	Na <sub>2</sub> O	K <sub>2</sub> O	LOI
Cement	21.29	4.18	62.28	3.34	2.64	2.40	0.13	0.59	2.09
Silica fume	88.29	0.14	0.92	0.19	1.51	3.21	0.14	0.17	5.26
Fly ash	54.69	12.71	17.48	4.61	0.97	1.68	1.75	3.18	1.79
LWA	65.46	16.75	1.08	7.63	0.45	2.43	3.82	0.94	0.27

### 18 **2.2 Specimens preparation**

19

1

Table 2 Mix proportion of the UHPC (kg/m<sup>3</sup>)

Num.	Cement	Silica fume	Quartz sand	Fly ash	LWA	Superplasticizer	w/b
C0	720	160	1250	80	0	9.60	0.180
C0-1	720	160	1250	80	0	9.60	0.185
C0-2	720	160	1250	80	0	9.60	0.190
C0-3	720	160	1250	80	0	9.60	0.195
C0-4	720	160	1250	80	0	9.60	0.200
C0-5	720	160	1250	80	0	9.60	0.205
C0-6	720	160	1250	80	0	9.60	0.210
C0-7	720	160	1250	80	0	9.60	0.203
C1	720	160	1000	80	150	9.60	0.196
C2	720	160	750	80	300	9.60	0.211
C3	720	160	500	80	450	9.60	0.227
C4	720	160	250	80	600	9.60	0.243

2

3 The mixture proportion of UHPC is shown in Table 2. The LWA was used to  
4 replace quartz sand. Before use, it was presoaked in water for 24 h. The mix process  
5 was adjusted when LWA was added. Firstly, the cementitious materials should be mixed  
6 with water and saturated LWA for 3 min. Then, the quartz sand was added and mixed  
7 for another 3 min. The contents of LWA were calculated based on the volume  
8 replacements of quartz sand. In this study, the UHPC mixtures with w/b ratios of 0.180,  
9 0.185, 0.190, 0.195, 0.20, 0.205 and 0.210, were prepared for slump flow test. Also, the  
10 UHPCs with an initial w/b ratio of 0.180 and different amounts of LWA were prepared  
11 to investigate the water desorption process of LWA. As different amounts of LWA were  
12 incorporated into the mixtures, the real w/b in Table 2 referred to the mass ratio of total  
13 water (including the additional water brought by saturated LWA) to binders. The cast  
14 UHPC specimens containing different amounts of LWA were sealed with plastic films



---

1 to prevent moisture exchange and cured at the temperature of 20°C. These specimens  
2 were measured with relative humidity, pore structure and mechanical properties.

### 3 **2.3 Methods**

#### 4 (1) Hydration characteristics

5 The heat flow and cumulative heat of samples with and without LWA were  
6 monitored by using an isothermal calorimetry (model TAM Air, Thermometric). The  
7 test temperature was  $20^{\circ}\text{C} \pm 0.1^{\circ}\text{C}$ . The samples were tested at 2 h after mixing with  
8 water. Each sample contained about 5 g of dry binders. The testing time lasted for 72 h.

9 The non-evaporable water content of samples without LWA and with  $450\text{kg}/\text{m}^3$  of  
10 LWA at 1d, 3d, 7d, 14d and 28d of curing were measured. The method was usually used  
11 to evaluate the degree of hydration of cementitious materials[10]. The samples from the  
12 middle of UHPC were grounded and dried in an oven at  $105^{\circ}\text{C}$  until the measuring mass  
13 was constant. Then, the powdered samples were heated at  $1050^{\circ}\text{C}$  for 3 hours. Usually,  
14 the mass loss difference between  $105^{\circ}\text{C}$  and  $1050^{\circ}\text{C}$  is considered as non-evaporable  
15 water. Meanwhile, the loss on ignition of binders was considered. Three replicates of  
16 each group were used to calculate the average value.

#### 17 (2) Free water content

18 The free water contents of UHPC at different ages were measured by freeze drying  
19 under vacuum. The UHPC samples with  $450\text{ kg}/\text{m}^3$  of LWA and without LWA were  
20 prepared and cured at  $20^{\circ}\text{C} \pm 0.1^{\circ}\text{C}$  under sealing condition. Each sample was placed  
21 into freeze dry condition at 30 min, 6 h, 12 h, 18 h, 24 h, 3 d, 7 d, 14 d and 28 d. When

---

1 the mass of sample was constant, the mass loss due to freeze drying was considered as  
2 free water content.

3 (3) Internal relative humidity

4 Specimens with size of 100 mm × 100 mm × 100 mm were prepared for internal  
5 relative humidity test. A hole was reserved in each specimen by placing a plastic sleeve  
6 at a depth of 50 mm, and the wall of sleeve was removed and packaged by polyester  
7 net fabric. A sensor was put into the hole to monitoring the RH and temperature. The  
8 accuracies of the measurement of RH and temperature are ±0.1% and 0.1°C. The  
9 measurement started at 15 min after mixing with water. The illustration of this  
10 measurement was shown in Figure 1.

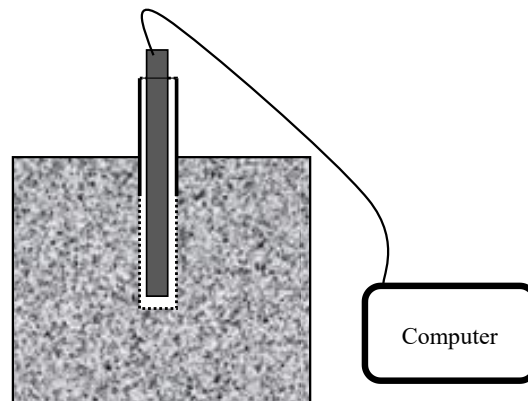


Figure 1 The illustration of relative humidity measurement

11 (4) Autogenous shrinkage and chemical shrinkage

12 The autogenous shrinkage was measured by a non-contact shrinkage deformation  
13 tester (model CABR-NES) according to the Chinese standard [37]. The specimens were  
14 covered with polyethylene film during testing. The autogenous shrinkage measurement  
15 was carried out after setting, the testing interval was 1 min. The chemical shrinkage

---

1 was tested according to the dilatometry in ASTM C 1068 [38]. The drop in the level of  
2 water in a hydrating UHPC was measured by a pipette, the volume change of water was  
3 regarded as the chemical shrinkage of UHPC. The measurement was started at 1 h after  
4 mixing with water

#### 5 (5) Pore structure

6 The pore structure of the UHPC with and without LWA were determined using  
7 nitrogen adsorption method. The specimens with the curing age of 12 h, 24 h, 3 d, 7 d  
8 and 28 d were tested. Before testing, the specimens were dried at 60°C. The mercury  
9 intrusion porosimetry (MIP) and nitrogen adsorption method were used to test the pore  
10 structure of LWA. The AutoPore IV 9500 series pore size analyzer (Micromeritics  
11 Instrument Corporation) was used for MIP method. The minimum and maximum  
12 pressures were 0.3 MPa and 414 MPa, respectively. A BELSORP-mini II made by  
13 Dutch Ankersmid company was used to measure the nitrogen adsorption and desorption  
14 isotherms.

#### 15 (6) Workability

16 The slump flow of UHPC with 450 kg/m<sup>3</sup> of LWA and without LWA was tested  
17 according to Chinese test method for fluidity of cement mortar (GB/T2419-2005) [39].  
18 In order to determine the water desorption before setting, the slump flow was tested at  
19 5 min, 30 min, 60 min, 90 min, 120 min and 180 min. The slump flow of samples with  
20 different initial water to binder ratios of 0.185, 0.19, 0.195, 0.20 and 0.21 were tested  
21 at 30 min and 180 min. The slump flow of UHPC containing 150 kg/m<sup>3</sup>, 300 kg/m<sup>3</sup> and  
22 600 kg/m<sup>3</sup> of LWA was also tested at 30 min and 180 min.

---

1 (7) LWA water absorption

2 The water sorption of LWA was assessed by wild-mouth bottle and pipette. This  
3 method was similar to a previous method by using volumetric flask [35]. Figure 2 shows  
4 the diagrammatic sketch of this setup. The LWA was firstly dried at 105°C, and 100g  
5 LWA was placed in a wild-mouth bottle (250ml). The water was filled to achieve nearly  
6 100% of capacity of the wild-mouth bottle and pipette, then it was vibrated for about 3  
7 min to eliminate air bubbles among LWA particles. Finally, the scale of water level was  
8 recorded at 5 min, 30 min, 1 h, 2 h, 3 h, 4 h, 5 h, 6 h, 7 h, 8 h, 9 h, 10 h, 11 h, 12 h, 13  
9 h ...24 h. The absorbed water can be obtained by calculating the water recorded at  
10 different time. After that, the water absorption of LWA with a function of time can be  
11 obtained.

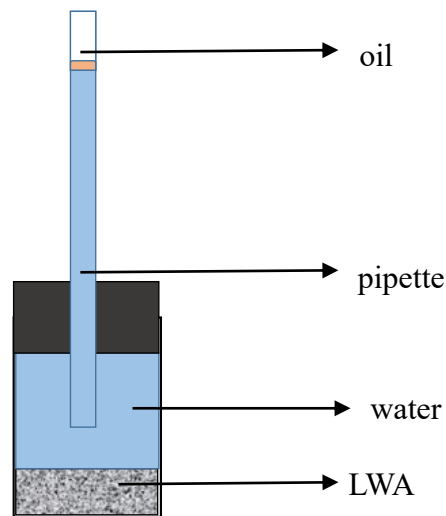


Figure 2 The diagrammatic sketch of setup to measure water absorption of LWA

12 (8) Water desorption capability

13 The water desorption of LWA can be described by the mass loss with a function of  
14 RH. A thermal-humidity test chamber was used to control the RH evolution. Before  
15 testing, the LWA was firstly dried at 105°C for 24 h and placed in tap water for 24 h

---

1 prior to testing. Then the LWA was patted to saturated-surface-dry and placed into  
2 thermal-humidity test chamber (RH 100% and temperature  $20^{\circ}\text{C}\pm 0.1^{\circ}\text{C}$ ) until the LWA  
3 achieved a constant mass. After the mass loss of sample was constant, the RH was  
4 changed in 1% steps to 90% [35, 40]. The mass loss was recorded, then the samples  
5 were dried at  $105^{\circ}\text{C}$  to obtain the total water absorption.

6 The free water evaluation of LWA under the RH development of UHPC with and  
7 without LWA was also tested. The saturated-surface-dry LWA was placed in to a  
8 thermal-humidity test chamber. The temperature of the chamber was kept at  $20\pm 0.1^{\circ}\text{C}$ .  
9 The RH evolution curves were set up according to the internal RH development of  
10 UHPC with  $450\text{kg}/\text{m}^3$  of LWA and without LWA. The mass loss of LWA at different  
11 curing ages was measured.

#### 12 (9) X-ray microtomography (CT)

13 An X-ray micro-CT scanner produced by Bruker CO., Ltd was used. The number  
14 of pixels in each section was  $1024\times 1024$  corresponding to  $4\ \mu\text{m}\times 4\ \mu\text{m}$  for each pixel.  
15 The specimens were prepared with a polypropylen pipe with a diameter of 2 mm. After  
16 mixing, the UHPC mixture with LWA was cast into the pipes. The pipes were sealed  
17 until the testing date and placed on the table of micro-CT machine. It should be noted  
18 that the LWA used in this study was saturated by CaI solution (the solubility is  
19  $150\text{g}/100\text{g}$  water). The same position of the sample was scanned at 6 h, 12 h, 24 h and  
20 168 h. There were 1500 projection directions used in different scans. The average  
21 projection data was used for image reconstruction algorithm based on a filtered back-  
22 projection method [41].

#### 23 (10) Mechanical properties

24 The UHPC specimens containing different amounts of LWA were casted for

---

1 compressive strength measurement. The size of specimens was 40 mm×40 mm×160  
2 mm. The specimens were demolded at 1 d and cured at 20±0.1°C under sealing  
3 condition. The compressive strength was tested with a loading rate of 2.4 kN/s at the  
4 age of 3d, 7d and 28d. Three specimens were performed to calculated the average  
5 value.

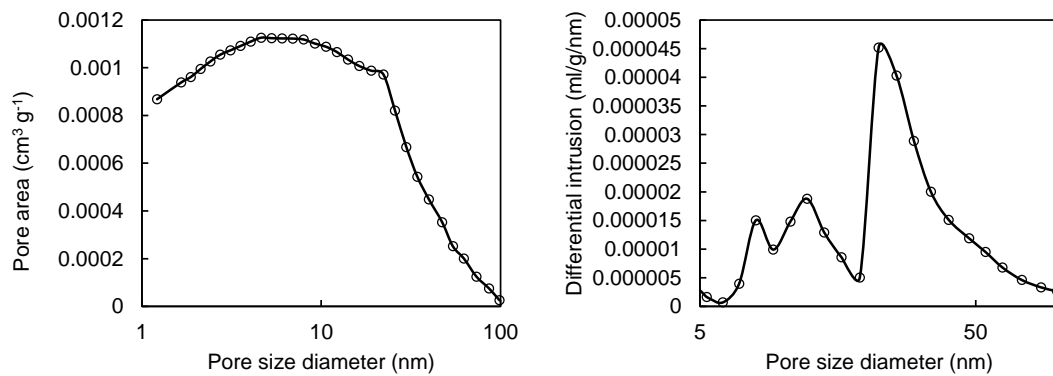
## 6 **3. Results and discussion**

### 7 **3.1 LWA characterization**

#### 8 **3.1.1 The pore structure of LWA**

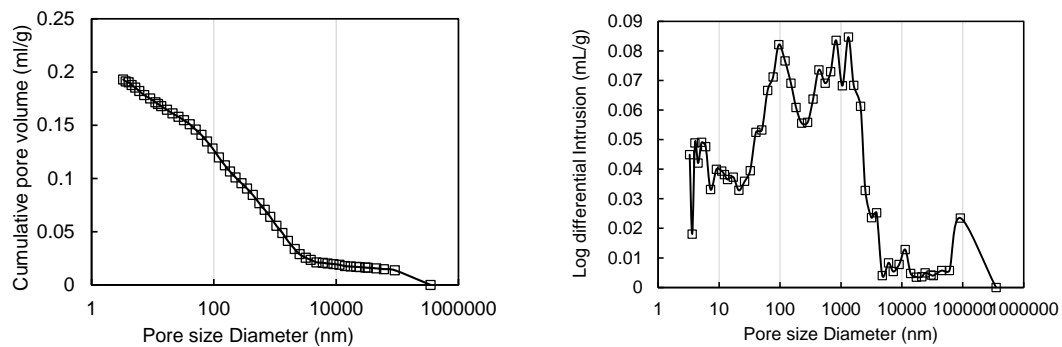
9 The pore structure of LWA was measured by nitrogen adsorption and MIP methods.  
10 The test results are shown in Figures 3 and 4 respectively. From the MIP results, the  
11 cumulative pore volume is 0.193ml/g. The pore size distribution shows that there are  
12 two peaks between 10 nm and 5000 nm, and a large number of pores with a size less  
13 than 100 nm can also be observed. However, the nitrogen adsorption test results show  
14 that the number of connective pores below 100 nm is low. As the nitrogen adsorption is  
15 nondestructive method, it can represent the fine pore structure accurately. Therefore,  
16 the pore structure obtained from MIP method seems to be incorrect, especially for the  
17 fine pores. Meanwhile, the porosity from MIP method is much higher than the actual  
18 porosity. It is likely that some non-connective pores in LWA are destroyed by pressure,  
19 and the pore structure is collapsed during testing. In addition, some macropores in LWA  
20 are presented as nano-pores in MIP test results, which is also related to the effect of ink-  
21 bottle pore [42]. Therefore, the MIP method may not be used to indicate the pore  
22 structure of LWA accurately. Considering the pore structure tested by these two methods,

1 it can be concluded that the size of the main pores in LWA are larger than 100 nm, which  
 2 is much larger than the main capillary pores in UHPC. Previous studies have indicated  
 3 that the water will move from coarser pores to finer pores during drying [35, 43]. So  
 4 the water in LWA will preferentially move from the LWA to the cement paste. This pore  
 5 structure characteristic of the LWA indicates that the water in these coarse pores will be  
 6 released into matrix easily during hydration. In order to evaluate the water desorption  
 7 ability of LWA in UHPC, the water absorption and water desorption capability of LWA  
 8 should be measured.



(a) The cumulative pore volume (b) The differential intrusion

Figure 3 The nitrogen adsorption test results of LWA



(a) Cumulative pore volume (b) Log differential intrusion

Figure 4 The MIP test results of LWA

---

### 1 **3.1.2 Water absorption of LWA**

2       The water absorption capability of LWA in UHPC is closely related to the effect  
3 of LWA on the mechanical properties, workability, hydration, autogenous shrinkage and  
4 durability [29, 44, 45]. Excessive and insufficient water absorption may lead to poor  
5 internal curing effect on the performance of concrete, for example, the reduction of  
6 mechanical properties and durability [35]. The water absorption process of LWA was  
7 tested by the device shown in Figure 2. The water absorption capabilities of LWA of  
8 different particle sizes are present in Figure 5. The water absorption of LWA is  
9 obviously influenced by the particle size. In fact, the water absorption increases with  
10 the increasing size of LWA. Larger LWA have larger porosity, and the voids become  
11 coincide with the fracture surface. The low capability of water absorption can be  
12 observed while the porosity decreases. The water absorption is rapid during the first 3  
13 h, which is due to absorption force from emptying pores in LWA. The water absorption  
14 still proceeds with a decreasing rate between 3 h and 24 h. The water absorption rate of  
15 LWA with size of 0.15-1.18mm is 10.1% at 24 h. After that, the water may still get into  
16 the LWA, and the LWA becomes over-saturated. But the water absorption rate at 24 h  
17 is used for mixture design [46]. In general, the LWA used in this study possesses a  
18 relatively high water absorption capability and shows potentials to be an ideal internal  
19 curing material. The amount of additional water and amount of LWA required for  
20 internal curing is closely related to its absorption capability. Thus, the proportion of  
21 LWA used in this study and the actual water to binder ratio is calculated based on the



1 water absorption capability.

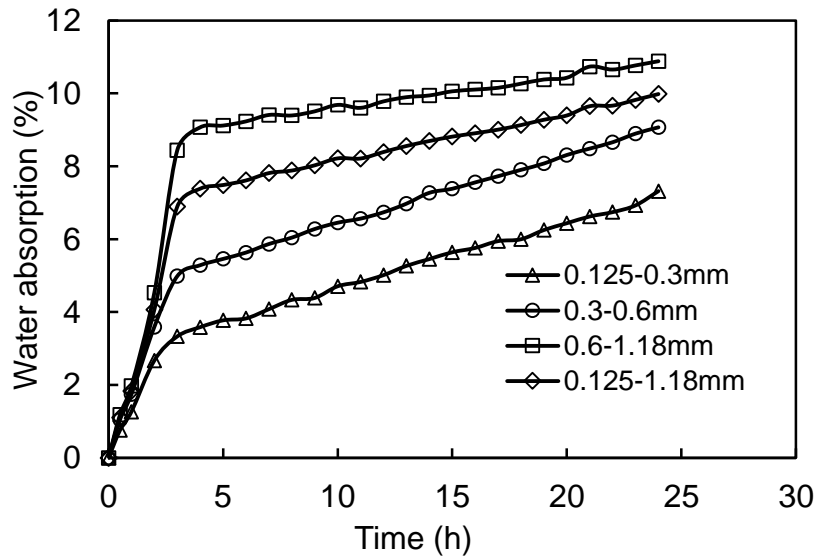


Figure 5 The water absorption process of LWA

### 2 3.1.3 Water desorption of LWA

3 Figure 6 shows the development of mass loss of saturated LWA vs. time. It can be  
4 seen from Figure 6 that the water content decreases rapidly with the decreasing RH.  
5 The change of mass decreases when the LWA approaches to equilibrium. Then, the  
6 mass loss at each RH decreases with the decreasing RH. This would be consistent with  
7 the volume and size of pores that water is lost. It should be noted that the majority of  
8 water has been released at very high RH. It can be seen from Figure 6 that more than  
9 half of entrained water has already been released at 99% RH, and about 94% of total  
10 entrained water in LWA has been desorbed at 98% RH. This indicates that most of the  
11 absorbed water releases at relatively high RH. Usually, the water in LWA should be  
12 released at relatively high RH to participate in the hydration of cement [47]. Therefore,  
13 the LWA used in this paper is an efficient internal curing material, which can promote

- 1 the hydration of cement at the early age. The entrained water in LWA will release
- 2 rapidly and show internal curing effect on the UHPC.

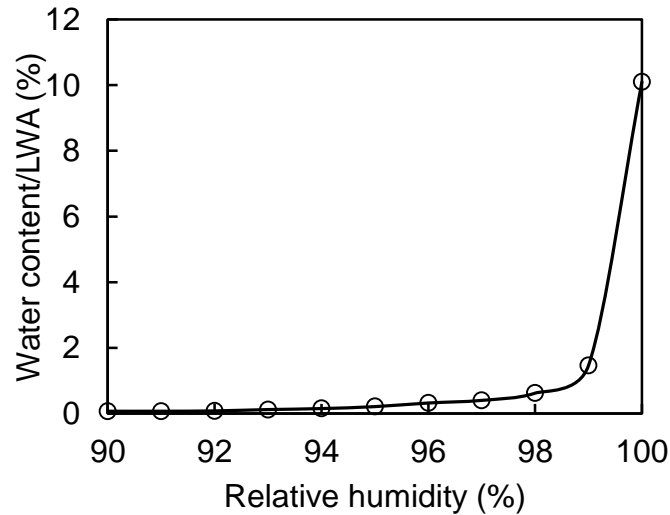


Figure 6 The water desorption behavior of the LWA

- 3 **3.2 Effect of LWA on the hydration, microstructure and**
- 4 **mechanical properties evolution of UHPC**
- 5 **3.2.1 Internal relative humidity and hydration characteristics**

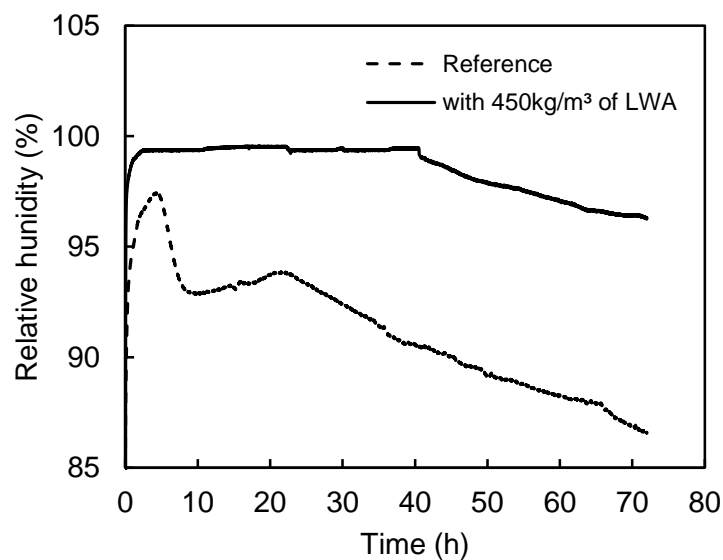


Figure 7 Internal relative humidity of UHPC with and without LWA

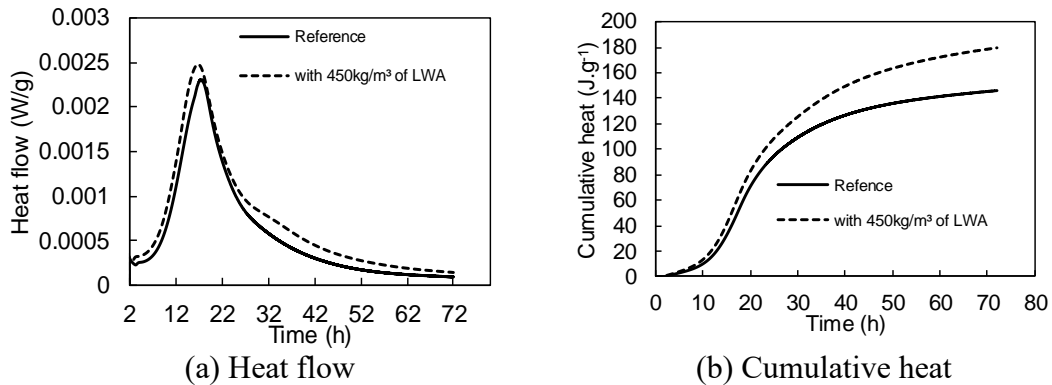
- 6 Figure 7 shows the internal RH vs. curing time of UHPC without LWA and with

---

1 450kg/m<sup>3</sup> of LWA. It can be observed that the RH is obviously improved, and the  
2 reduction of RH is delayed [21]. In addition, the UHPC with LWA exceeds a high RH  
3 of 99.3% at about 3 h and keeps the RH high. The increase of RH and non-reduction of  
4 humidity at early age is related to the water desorption of LWA. Actually, it is the  
5 entrained water from LWA makes the capillary pores saturated and improves the  
6 internal RH at the early age. It should be noted that much water has released before  
7 setting (before 6 h), which improves the RH at early age. This water is not for internal  
8 curing but increases the initial water to binder ratio of UHPC, which is expected to be  
9 adverse to the performance of UHPC.

10 The internal RH is rather low in reference UHPC due to the low water to binder  
11 ratio, as a result, a high self-desiccation is present. The maximum internal RH of  
12 reference sample is 97.4% at about 3 h. This means that some pores are empty even  
13 when the UHPC is still mixture. However, the water desorption of LWA improves the  
14 internal RH at early age, and the internal RH of UHPC mixture with LWA reaches to  
15 about 99.3% at 3 h, implying that the empty pores are nearly saturated. This further  
16 leads to the delay of occurrence of self-desiccation. Therefore, a low autogenous  
17 shrinkage will be found [19, 21]. From the development of internal RH, it can be  
18 concluded that the addition of LWA improves the internal RH of UHPC not only at early  
19 age but also that at later age. The improvement of RH owing to water desorption can  
20 truly reduce the autogenous shrinkage and risk of cracking. However, some water is  
21 released before setting when the UHPC is still mixture, which is unexpected and makes

1 negative influence on the performance.



(a) Heat flow (b) Cumulative heat  
Figure 8 Hydration heat release rate and cumulative heat of UHPC

2 Since the internal RH was changed by adding LWA, the hydration was sure to  
3 show some differences. Figure 8 shows the isothermal calorimetry heat curves of UHPC  
4 with  $450\text{kg/m}^3$  of LWA and without LWA. The hydration heat is obviously influenced  
5 by the water desorption of LWA. As the internal RH of UHPC mixture is increased after  
6 adding saturated LWA (shown in Figure 7), the heat flow before setting (before 6 h) is  
7 a little higher than that of reference sample. This also confirms that some water is  
8 released before setting, which increases the water to binder ratio of UHPC. For the age  
9 between 6 h and 24 h, the heat flow is also increased by adding LWA. The water  
10 desorption of LWA accelerates the hydration of cementitious materials during the first  
11 day [33, 48], but the cumulative heat shows little difference at the first 24 h. Moreover,  
12 there is a shoulder at the age between 24 h and 72 h (show in Figure 8(a)), showing a  
13 higher heat flow compared to reference sample. The improvement of heat flow and  
14 cumulative heat is closely related to the water released from LWA. This indicates that  
15 much water is released at the age between 24 h and 72 h. From the isothermal  
16 calorimetry heat results, it can be seen that water desorption in LWA plays an important

---

1 role in controlling the hydration of UHPC. The water released from LWA improves the  
2 internal RH and further influences the hydration process. It should be noted that the  
3 internal curing effect become significant after the first day, owing to the rapid decrease  
4 of internal RH of reference sample. From the hydration heat evolution, the hydration is  
5 closely related to water desorption behavior of LWA, the water released from LWA not  
6 only improves the hydration during the first day but also promotes the hydration in the  
7 following stage, indicating a continuous water desorption process of LWA. The increase  
8 of hydration heat implies the improvement of hydration degree, which may bring the  
9 enhancement of pore structure.

10 In addition, in order to evaluate the influence of LWA on the degree of hydration,  
11 the non-evaporable water content of samples without LWA and with  $450\text{kg/m}^3$  of LWA  
12 at 1d, 3d, 7d, 14d and 28d of curing were measured. The test results show that the water  
13 desorption increases the degree of hydration at early and later stages of curing. As the  
14 additional water to binder ratio of C3 is 0.047, which is incorporated in the saturated  
15 LWA. The improvement of non-evaporable water content will be 26.1%, when all the  
16 additional water from LWA becomes chemical water. However, the actual improvement  
17 of non-evaporable water content at 28d is 13.4%, which is much lower than that the  
18 expected improvement of non-evaporable water content. The non-evaporable water  
19 content is commonly used to evaluate the degree of hydration of cementitious materials,  
20 and the increase of non-evaporable water content is equal to the development of degree  
21 of hydration. Generally, the degree of hydration is obviously increased by adding LWA.

The improvement of degree of hydration may change the pore structure of matrix and further influence the mechanical properties.

Table 3 The non-evaporable water content

Time (d)		1	3	7	14	28
Non-evaporable water	reference	0.118	0.121	0.135	0.139	0.144
content (g/g binder)	With 450kg/m <sup>3</sup> of LWA	0.123	0.128	0.153	0.157	0.163
Improvement (%)	With 450kg/m <sup>3</sup> of LWA	4.95	5.83	13.05	13.29	13.39

### 3.2.2 Evolution of pore structure

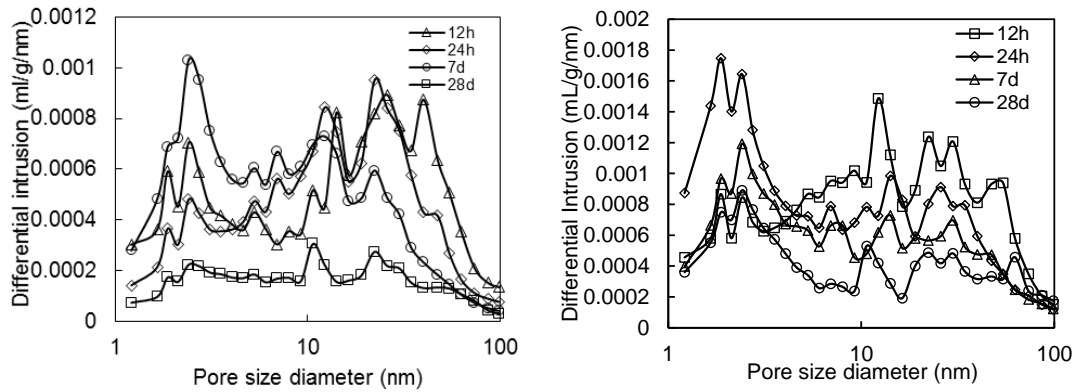
The pore structure of UHPC (without and with 450kg/m<sup>3</sup> of LWA) were tested by nitrogen adsorption method. As the main pores in LWA are larger than 100 nm, the influence of porous LWA on the test results can be neglected. The test results can represent the pore structure of the matrix. Figure 9 shows the pore size distribution of UHPC at different stages of curing. It can be observed that the development of pore structure of UHPC with and without LWA (Figure 9) both show decreasing trends, but there are still some differences in pore size distribution and variation process. As is shown in Figure 10, the porosities of both samples decrease rapidly with the increasing curing age, but the reduction of porosity of UHPC containing LWA is more significant than that of reference sample. It should be noted that the reduction rate increases with the increasing stages of curing. In addition, the porosity of UHPC with LWA is 0.0638cm<sup>3</sup>/g at 12 h, indicating a higher porosity than that of reference sample. Generally, the water to cement ratio is one of the important factors influencing pore

---

1 structure, and the porosity will be increased and pores can be coarsen by improving the  
2 water to cement ratio [49]. Because the internal RH in UHPC mixture is very low  
3 (shown in Figure 6), the water in LWA is released after mixing due to RH gradient. The  
4 initial water to binder ratio thereby is increased. Therefore, it can be concluded that  
5 some water stored in LWA may be released when the UHPC is still with the state of  
6 mixture, leading to an increasing water to binder ratio. But the internal curing of LWA  
7 offsets this disadvantage in the following ages, as a result, the porosity of UHPC  
8 containing LWA is lower than that of reference sample at 24 h. Also, the reduction rate  
9 becomes more and more obvious as the curing age increases. Besides, the pore size  
10 distribution and its development of UHPC is significantly changed. The volume of  
11 coarse pores (>50 nm) is reduced by internal curing of LWA, but the amount of pores  
12 with the size below 50 nm shows an opposite trend. This indicates that the internal  
13 curing of LWA not only reduces the coarse pores but also increases the fine pores at  
14 different ages. Therefore, the average pore size is reduced due to internal curing. It is  
15 worth noting that the differences in proportion of fine pores (<50 nm) become more  
16 and more obvious with the increasing curing age, which means that the proportion of  
17 fine pores increases continuously compared to that of reference sample.

18 Based on the above analysis, the water desorption of LWA is closely related to the  
19 development of pore structure. The water desorption before setting shows an adverse  
20 effect on the porosity as well as the distribution of pore structure. But as the water  
21 desorption proceeds, this effect is overwhelmed by the beneficial effect of internal

1 curing. In general, the evolution of pore structure is closely related to the water  
 2 desorption behavior of LWA in UHPC.

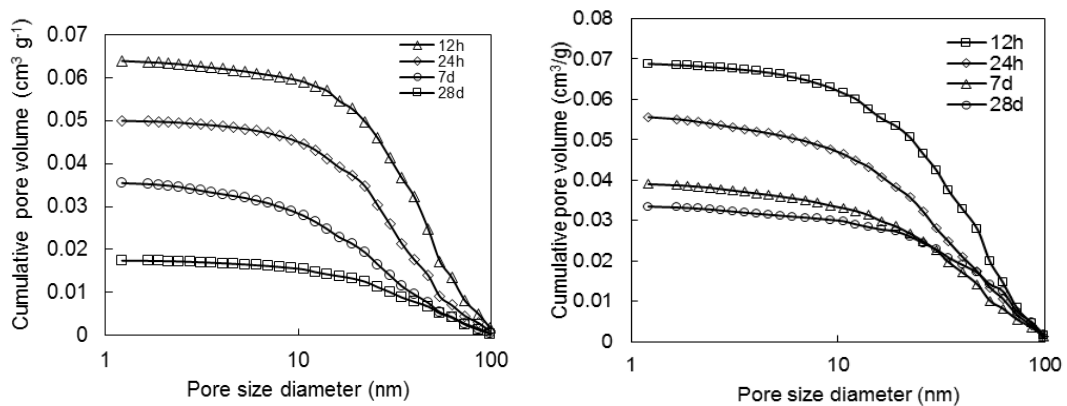


(a) with 450kg/m<sup>3</sup> of LWA

(b) without LWA

Figure 9 The pore structure distribution of UHPC with and without LWA

3



(a) with 450kg/m<sup>3</sup> of LWA

(b) without LWA

Figure 10 The cumulative pore volume of UHPC with and without LWA

4

### 5 3.2.3 Evolution of mechanical properties

6 The development of compressive strength of UHPC with 450kg/m<sup>3</sup> of LWA and  
 7 without LWA is shown in Figure 11. The test results indicate that the compressive  
 8 strength of UHPC containing LWA is lower than that of reference sample at early age  
 9 (3 d), but it exhibits a higher compressive strength than that of reference sample at the



---

1 age of 7 d and 28 d. Compared with the reference sample, the compressive strength  
2 increases by 6.0% at 28 d when the 450kg/m<sup>3</sup> of LWA is presented. It should be noted  
3 that the 3d-compressive strength is reduced by adding LWA, which is due to the water  
4 desorption of LWA before setting and the high porosity of LWA. Although the matrix  
5 of UHPC containing LWA possesses a lower porosity than that of reference sample at  
6 24h, the total porosity is obviously increased by porous LWA, leading to the reduction  
7 of mechanical properties. As the internal curing is on-going in the later time, the  
8 enhancement of matrix from internal curing overwhelms the initial disadvantages of the  
9 water desorption before setting. Therefore, the compressive strength of UHPC  
10 containing LWA is higher than that of reference samples at 7 d and 28 d.

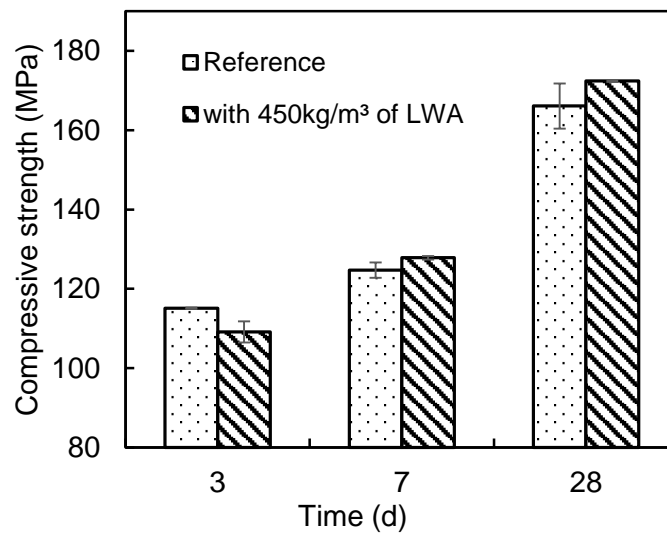


Figure 11 The compressive strength of UHPC containing different LWFA

---

## 1 **3.3 Water desorption process of LWA in UHPC**

### 2 **3.3.1 Free water evaluation**

3 The free water evolutions of UHPC with and without LWA were measured to  
4 indicate the water desorption process of LWA in UHPC. The development of free water  
5 content of UHPC is shown in Figure 12. The experimental results show that the free  
6 water in UHPC with and without LWA is consumed rapidly during the first 24 h. But  
7 the difference in water content between UHPC with 450kg/m<sup>3</sup> of LWA and without  
8 LWA diminishes with increasing stage of curing. It is worth noting that the amount of  
9 the free water becomes similar at 14 d. This indicates that the free water stored in LWA  
10 is almost exhausted at 14 d.

11 During the first 24 h, there is about 15.34% free water that has been consumed in  
12 UHPC with LWA, which is much higher than that of reference sample (11.64%). The  
13 left free water content is 7.90% and 6.74% at 24h, which is corresponding to UHPC  
14 with and without LWA, respectively. This indicates that much moisture stored in LWA  
15 has released and participates in the hydration of cement paste during the first 24 h. From  
16 the pore structure shown in Figure 9 and Figure 10, these two samples possess similar  
17 porosity at about 12 h. But the water desorption of LWA promotes the hydration and  
18 reduces the porosity in the following curing age. Compared to the reference sample, the  
19 water released from LWA is at least 3.70% during the first 24 h, 0.50% between 24 h  
20 and 3 d, 0.63% between 3 d and 14 d and 0.12% between 14 d and 28 d, respectively.  
21 Much water releases into pores of UHPC, but it is difficult to distinguish from the total

1 free water. Therefore, it can be obtained from the evolution of free water, at least 76.00%  
 2 of total water presoaked in LWA has been released at 24 h. Also, there is much water  
 3 that participates in the hydration between 24 h and 14 d. After that, the water in LWA  
 4 is almost exhausted, and the free water content in UHPC with and without LWA  
 5 becomes similar. Therefore, it can be observed from the test results that most of water  
 6 in LWA has been released at the early age, and this water fills into the empty pores and  
 7 promotes the hydration of UHPC and reduce the autogenous shrinkage.

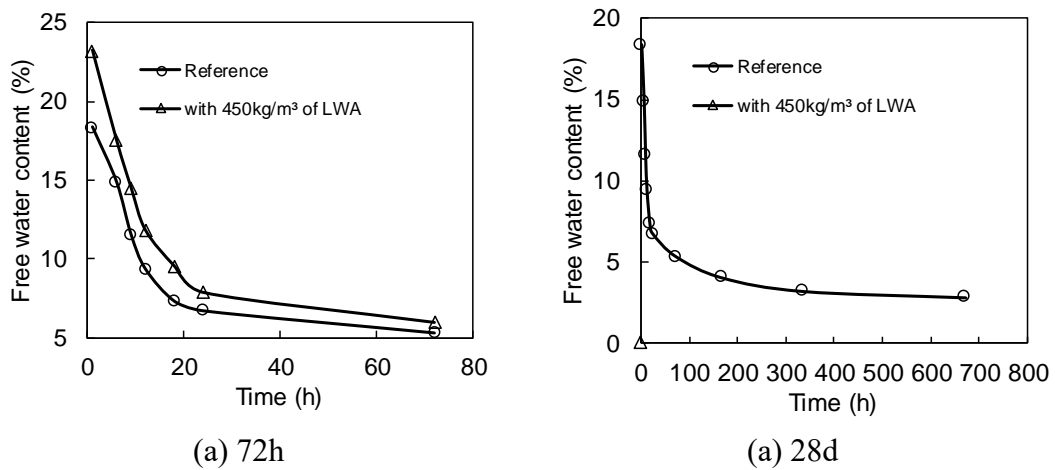


Figure 12 Free water content evolutions of UHPC with and without LWA

### 1 3.3.2 Water desorption of LWA under the RH evolution of UHPC

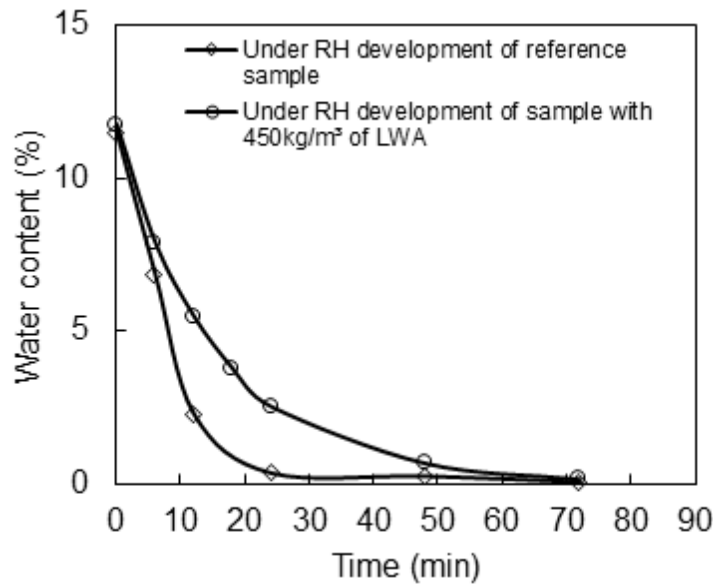


Figure 13 The water desorption of LWA under RH evolution of UHPC

2 The water desorption curves of wet LWA under RH development of samples with  
3 and without LWA are plotted in Figure 13. The test results show that the water releases  
4 rapidly during the first 20 h. Because the maximum value of internal RH curve of  
5 reference sample is only 97.4%, decreases quickly after 6 h and approximately 80.0%  
6 of total water has been released during first 12 h. Then, the water desorption slows  
7 down in the following time, and more than 95.0% of water has released at 24 h. After  
8 that, the water releases slowly in the following time. However, the water release is  
9 significantly reduced when the RH is improved (under RH development of sample with  
10 450kg of LWA). Therefore, the differences in water desorption of these two curves are  
11 mainly depended on internal RH development. Compared to the water release in  
12 ordinary concrete [26], the low RH accelerates the desorption of water in LWA.

---

1 For the UHPC without LWA, it is possible that the water saturated in LWA releases  
2 rapidly when it is still mixture. This is mainly driven by the RH gradient. This water  
3 desorption before setting is adverse to the microstructure and mechanical properties due  
4 to increasing water to binder ratio. Moreover, the internal RH is significantly increased  
5 by adding saturated LWA, so the motivation from RH gradient is expected to be  
6 weakened. Actually, the water desorption of LWA in UHPC depends on not only on the  
7 RH gradient but also the pressure of capillary pores [36]. The actual water desorption  
8 can be accelerated by capillary pressure, but the decreasing RH gradient (relatively high  
9 internal RH) will reduce the influence of capillary pressure. Therefore, the water  
10 desorption of LWA in UHPC will be rapid in the first 3 h, but the water desorption  
11 would be slow down due to the relatively high RH. This water desorption in UHPC is  
12 expected to be more rapid than the measured water desorption of LWA under the RH  
13 evolution of UHPC, owing to the presence of capillary pressure.

### 14 **3.3.3 Workability**

15 The above results indicate that some water in LWA has been released before setting.  
16 In the previous study, the desorption behavior of SAP could be evaluated by comparing  
17 the rheology [18]. In order to evaluate the water desorption of LWA in UHPC mixture,  
18 the workability of UHPC mixtures with and without LWA were measured. It can be  
19 observed from Figure 14 that the slump flow changes complexly with function of time.  
20 Firstly, both slump flow curves increase during the first 30 min, which is attributed to  
21 the delay dispersion of superplasticter [50]. After that, for reference UHPC, the slump

---

1 flow decreases gradually due to hydration [51]. However, the sample with LWA shows  
2 an opposite trend compared to the reference sample. Although the hydration is adverse  
3 to the workability of UHPC containing LWA, the slump flow still shows an unexpected  
4 increasing trend in the following 2 h. The slump flow increases from 225 mm to 290  
5 mm when the age proceeds from 5 min to 180 min. Meanwhile, the slump flow reaches  
6 to the maximum value at 150 min and then decreases. Apart from water desorption of  
7 LWA, it seems that there is no other reason leading to the increase of slump flow.  
8 Therefore, it should be concluded that a large amount of water is released during first 3  
9 h, which increases the water to binder ratio of UHPC. As a result, the workability  
10 increases with the curing age.

11 In order to obtain the amount of water that released before setting, the slump flows  
12 of UHPC with water to binder ratios of 0.185, 0.19, 0.195, 0.20, 0.205 and 0.21 were  
13 tested at different ages. The results tested at 180 min are shown in Figure 15. The slump  
14 flow increases with the increasing water to binder ratio. The relationship between slump  
15 flow and water to binder shows a linear relation. An equation describing the relationship  
16 between slump flow and water to binder ratio is given as following.

$$17 \quad S=2123.6w/b-141.53 \quad R^2=0.983 \quad (1)$$

18 where  $S$  is slump flow (mm);  $w/b$  is water to binder ratio of UHPC.

19 As the addition of LWA has little influence on the initial workability, the evolution  
20 of slump flow is mainly due to the water desorption. The water desorption of internal  
21 curing materials could be evaluated by comparing the rheology [18]. In this study, the

---

1 workability is used to quantify the amount of water desorption. From the relationship  
2 between slump flow and water to binder ratio, the slump flow of UHPC reaches 290  
3 mm when approximately 0.0203 extra water is added. This means that 49.4% of pre-  
4 soaked water in UHPC releases during the first 180 min. From the development of  
5 internal RH, the RH of UHPC with LWA is very high and keeps stable after 3 h.  
6 Meanwhile, the heat flow is slowly between 3 h and 6 h (shown in Figure 8). So, the  
7 water desorption between is expected to be little. Because it is difficult to obtain the  
8 amount of water released between 3 h and final setting time, the 49.40% of water  
9 released during the first 180 min can be identified as the water that is not for internal  
10 curing (the actual value is certainly higher than 49.40%). Therefore, the water released  
11 before setting accounts for high percent of total extra water, more attention should be  
12 paid to reduce the influence of this water.

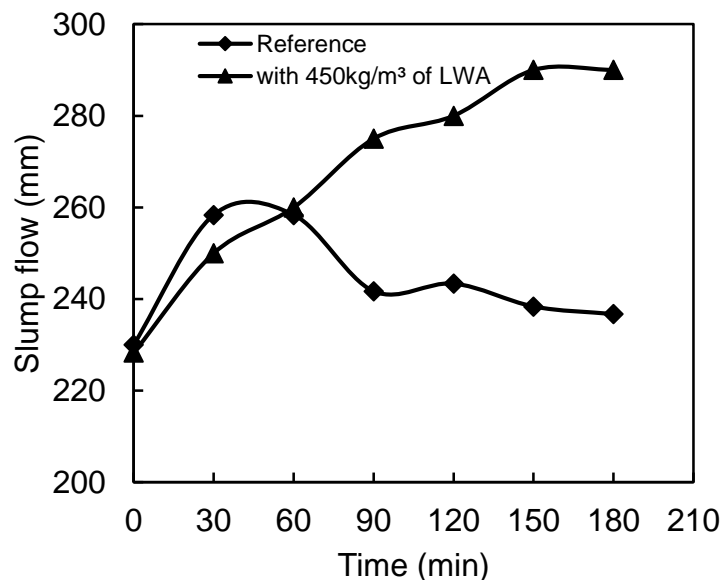


Figure 14 The slump flow of UHPC mixture with and without LWA

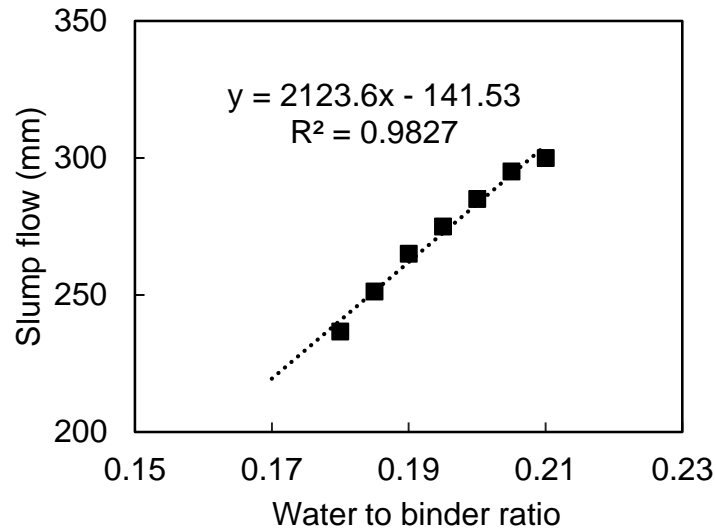


Figure 15 The effect of water to binder ratio on the slump flow of UHPC

### 1 3.3.4 In-situ observation of water desorption of LWA in UHPC

2 The micro X-ray CT scanner was used to determine the water desorption of LWA.

3 As both air voids and free water in concrete contribute to the porosity peaks [52]. The

4 CaI solution was used to distinguish pores containing free water from empty pores. The

5 samples were tested at 6 h, 12 h, 24 h and 7 d. The 2D-images at different ages for the

6 same position of UHPC are shown in Figure 16. The resolution ratio of this test is

7  $0.7\mu\text{m}/\text{voxel}$ . The CaI solution possess a higher grey level than water, so the grey level

8 of saturated pores in LWA is larger than 50. Usually, the grey level of empty pores is

9 below 46 [53]. It can be observed in Figure 16(a) that there are many large pores being

10 empty at 6 h, which indicates much water has been desorbed during the first 6 h.

11 Furthermore, the water in fine pores of LWA release quickly in the following time. As

12 the presence of CaI solution, the grey level of some parts of saturated pores is higher

13 than empty pores, the average grey level of LWA is about 58.2 (calculated from 100

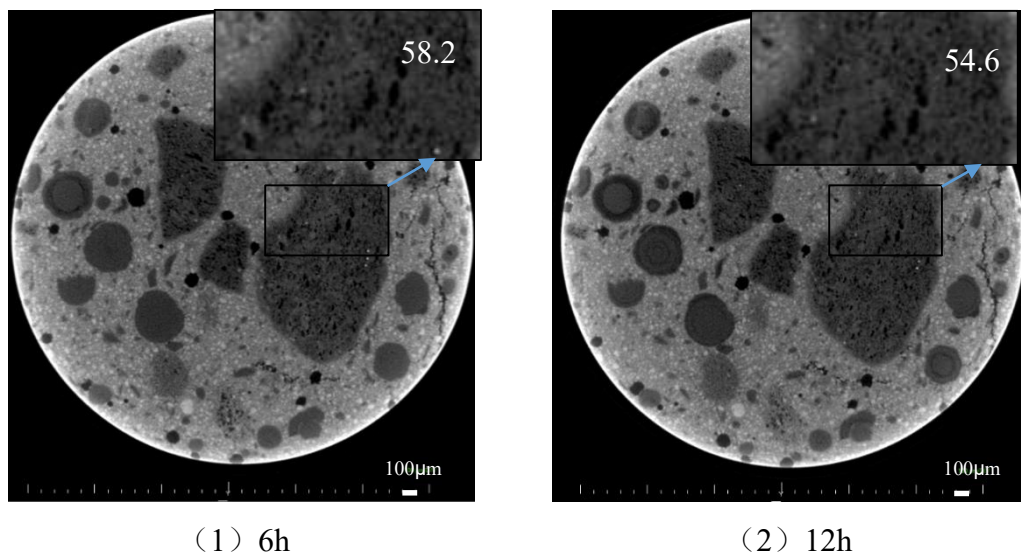
14 points in LWA) at 6 h, shows significant difference from empty pores. The average grey



---

1 level is rapid decreased to 45.5 at 24 h, representing large amount of water in LWA has  
2 released. However, the development of average grey level slows down from 24 h to 7  
3 d, and little difference can be obtained by calculating average grey level. Therefore,  
4 most of water in LWA has been desorbed during the first 24 h, after that there is little  
5 water remained in LWA. Also, it should be noticed that some CaI crystals are separated  
6 out in LWA at 7 d.

7 On the basis of the above qualitative observation, the slices obtained using  
8 tomography is an effective in situ method to indicate the water desorption of LWA. It  
9 can be concluded that the water in large pores of LWA desorbs rapidly before setting.  
10 So many large pores are empty at 6 h. The water in fine pores desorbs quickly during  
11 the period between 6 h and 24 h, and most of the water in LWA is already desorbed  
12 during the first 24 h. But these images from the same place of UHPC also illustrate the  
13 difficulty to achieve the transport process of moisture in cement paste and the actual  
14 remained water in LWA.



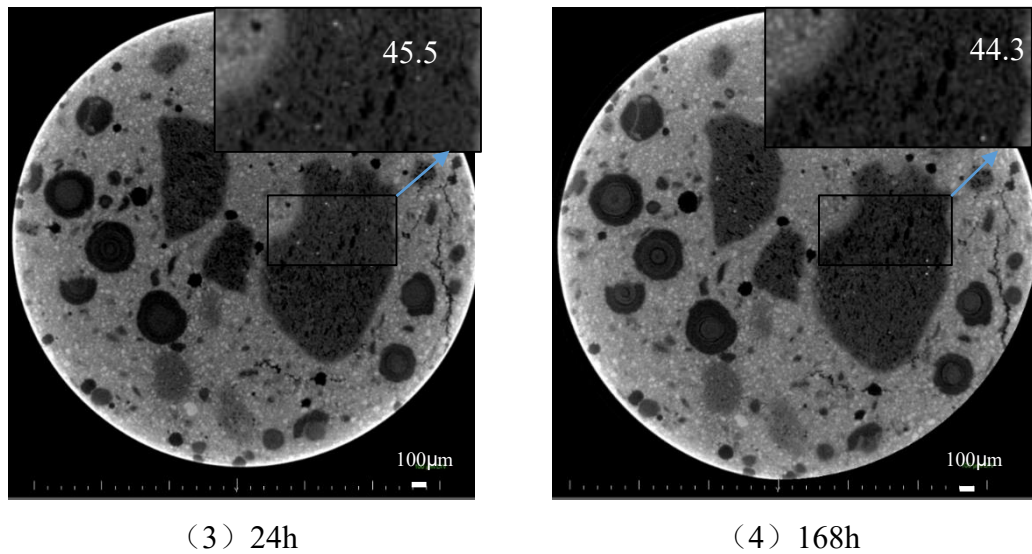


Figure 16 The micro-CT images of UHPC at different ages

### 1 3.3.5 Chemical shrinkage and autogenous shrinkage

2 As the water stored in LWA has been released before setting, the initial water to  
 3 binder ratio of UHPC containing  $450\text{kg/m}^3$  of LWA is equal to about 0.203. Therefore,  
 4 the UHPC with the water to binder ratio of 0.203 was prepared to determine its chemical  
 5 shrinkage and autogenous shrinkage. The test results are shown in Figure 17. From the  
 6 development of internal RH shown in Figure 7, the RH in UHPC containing LWA  
 7 indicates that the capillary pores keep saturated for about 40 h. About 0.017 water to  
 8 binder ratio is needed to fill into the void space created by chemical shrinkage. As the  
 9 pores in UHPC are still nearly saturated at 40 h in UHPC containing  $450\text{kg/m}^3$  of LWA,  
 10 the water released during the period between 6 h and 40 h is mainly used to fill in the  
 11 pores created by chemical shrinkage. Considering the water desorption before setting,  
 12 there is at least 0.04 extra water to binder ratio has already released at 40 h. In other  
 13 words, about 85.10% water stored in LWA has been released before 40 h. These results

1 are different from result obtained from thermal-humidity test chamber. Although the  
2 RH gradient is one of the most important factors that should be considered, the actual  
3 water desorption depends on many other factors such as pore structure and LWA content  
4 [54, 55].

5 According to previous study, as for ordinary and high performance concrete, the  
6 volume fraction of water migrating from LWA exhibited a one-to-one agreement with  
7 the measurement chemical shrinkage of cement paste [54], the water in LWA is  
8 completely used for internal curing. But for UHPC, nearly half of the water stored in  
9 LWA is not for internal curing. This may be the main difference between water  
10 desorption in UHPC and that of other concrete with high water to binder ratio.

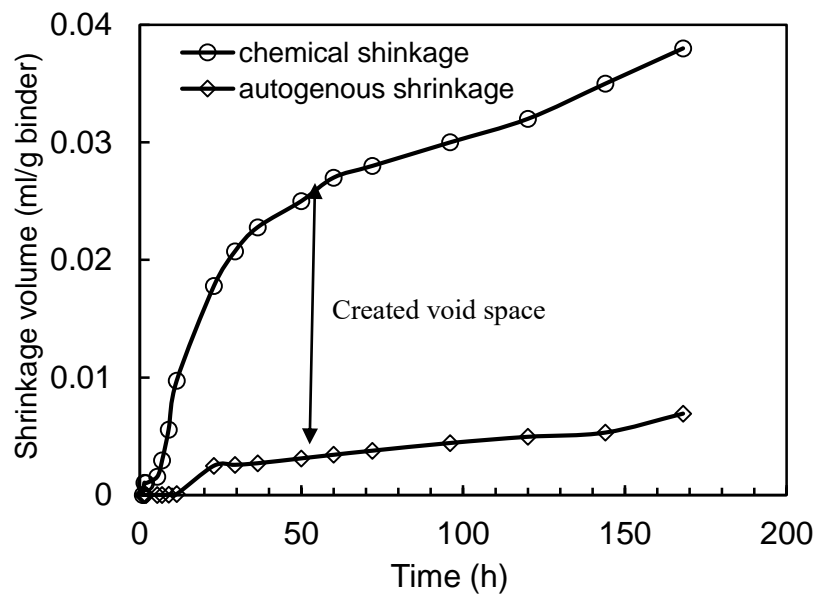


Figure 17 The chemical shrinkage and autogenous shrinkage of UHPC

---

## 1 **4. Further discussion**

### 2 **4.1 Characteristic water desorption of LWA in UHPC**

3       Based on the experimental results, the water desorption process of LWA in UHPC  
4 can be divided into 4 stages (shown in Figure 18). In the first stage, the saturated LWA  
5 is surrounded by UHPC mixture with low RH, and the water releases with high rate.  
6 This water desorption occurs before setting, which improves the initial water to binder  
7 ratio of UHPC. Because the UHPC is still mixture, the water desorption is mainly  
8 controlled by RH gradient. In the second stage, the internal RH is very high and the  
9 pores in matrix is nearly saturated, and the hydration rate is still slow. The UHPC is in  
10 the state of mixture, and no self-desiccation can be found, so the water desorption is  
11 slow, which shows limited influence on the water to binder ratio and hydration. In the  
12 third stage, it starts after the time of final setting, the water releases into the matrix and  
13 is used for internal curing. The RH keeps high during this period due to water desorption.  
14 But the water consumption of hydration is rapidly, leading to quick water desorption of  
15 LWA. The water desorption is possible to be motivated by capillary pressure rather than  
16 RH gradient, which is due to the relatively high and constant RH. In the fourth stage,  
17 most of water stored in LWA has been released. As the internal RH decreases with the  
18 increasing curing age. Apart from the RH gradient, the capillary pressure is very high,  
19 which promotes the desorption and migration of water in LWA. However, the porosity  
20 and connectivity of capillary pores in UHPC is continuously reduced [27], so the water

1 desorption and migration is gradually slowed down. So, there are three main factors  
2 controlling the water desorption of LWA in the fourth stage: internal RH, capillary pore  
3 pressure and pore structure.

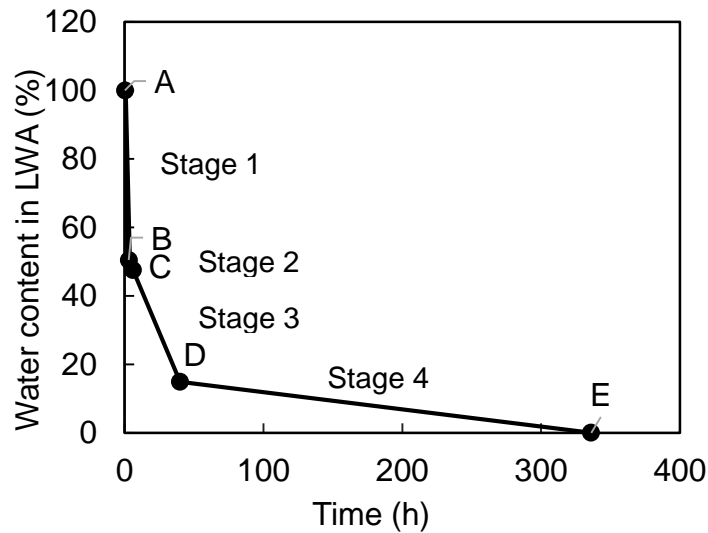


Figure 18 A characteristic desorption curve of LWA in UHPC

4 As is known to all, the pore structure of capillary pores in hardened concrete are  
5 closely related to the initial water to cement ratio and hydration degree [49]. Much  
6 water in LWA has been release before setting due to the very low water to binder ratio.  
7 This free water increases the initial water to binder ratio of UHPC which may be  
8 adverse to the mechanical strength and permeability of UHPC. This is usually mostly  
9 unexpected. If the water releases at too early age, for example, during the first stage,  
10 this free water is not for internal curing. Considering the internal curing effect of LWA,  
11 the water stored in LWA is expected to be released less in the first stage and more in the  
12 third and fourth stage, so that the LWA can bring better internal curing efficiency.  
13 Therefore, a kind of LWA with fine pore size may improve the internal curing efficiency.  
14 Because the water in coarse pore would release easily at high internal RH and low RH

---

1 gradient [24].

2        Nevertheless, the water desorption process of LWA in UHPC is individual due to  
3 the very low water to binder ratio and large amount of superfine powders. The water  
4 desorption behavior of LWA in UHPC is significantly different from that of normal  
5 concrete [36], and it can be showed as follows: Firstly, much water stored in LWA has  
6 been released before setting; Secondly, the water in LWA is released rapidly between 6  
7 h and 24 h, and most of the water has been released during the first day of hydration.

8        Based on the above analysis, the desorption process of LWA in UHPC is plotted  
9 in Figure 18. There are three inflection points at 3 h, 6 h and 40 h for UHPC containing  
10  $450\text{kg/m}^3$  of LWA. These three inflections are denoted as B, C and D, respectively.  
11 These three inflection points are related to the setting time of UHPC, the content and  
12 characteristic of LWA and mix proportion of UHPC. This curve is plotted as a linear  
13 line in each stage. However, every stage is not linear due to the evolution of RH and  
14 pore structure. Among these four stages, the water released during the first and second  
15 stage is not used for internal curing.

## 16 **4.2 The utilization rate of the internal curing water**

17        It can be observed from Figure 18 that the water desorption during the first and  
18 second stage is used to increase the water to binder ratio, which is not used for internal  
19 curing. As the water desorption in the second stage is slow due to high internal RH. The  
20 released water that is useless for internal curing refers to the water desorption in the

---

1 first stage (shown in Figure 18). It can be obtained from Figure 13 that much water has  
2 been released at 180 min, and an equation describing the relationship between slump  
3 flow (at 180 min) and the real water to binder ratio is given. Meanwhile, the addition  
4 of LWA has little influence on the initial workability of UHPC. If the slump flow (at  
5 180 min) and initial water to binder ratio are known, the additive water to binder ratio  
6 can be obtained by real water to binder ratio minus initial water to binder ratio.  
7 Therefore, the water desorption in the first stage can be known. Here, the utilization  
8 rate ( $U_{ic}$ ) of internal curing water of LWA is referred to the ratio of water desorption  
9 except the first stage to total pre-soaked water. The workability of UHPC containing  
10 different dosages of LWA is tested (shown in Figure 19) to calculate the utilization rate  
11 of internal curing water.

12 The  $U_{ic}$  of UHPC containing  $450\text{kg/m}^3$  of LWA is 50.6%, which is calculated  
13 based on the development of workability and Equation (1). Actually, the water to binder  
14 ratio and LWA content would influence the utilization rate. Figure 20 shows the effect  
15 of LWA content on the utilization rate of water stored in LWA. It can be observed that  
16 the utilization rate is very low for a low content of LWA ( $150\text{kg/m}^3$ ), most of the water  
17 in LWA has been released during the first stage. Although more water is introduced to  
18 UHPC when more saturated LWA is added, the proportion of water released in the first  
19 stage decreases with the increasing LWA content. In others words, the utilization rate is  
20 improved as the increasing LWA additions. The utilization rate of samples with  
21  $150\text{kg/m}^3$ ,  $300\text{kg/m}^3$ ,  $450\text{kg/m}^3$  and  $600\text{kg/m}^3$  of LWA are 27.35%, 42.56%, 50.60%

---

1 and 55.70%, respectively. This means that more water stored in LWA is released in  
2 sample with higher LWA content during the third and fourth stages. However, it should  
3 be noted that different additions of LWA in this study cannot meet the required  
4 theoretical water amount, so even 75% LWA would not be enough for shrinkage  
5 compensation [19]. For all the samples, no matter how much LWA is present, much  
6 water will be released before setting, which increases the workability and water to  
7 cement ratio. This is adverse to the microstructure and mechanical performance of  
8 UHPC. A higher  $U_{ic}$  is found in sample with higher LWA content. Also, it can be  
9 observed in Figure 14 and 16 that much water has been released at early age, and the  
10 coarse pores are empty at 6 h. In order to further improve the  $U_{ic}$ , improving the LWA  
11 additions and reducing the pore size of LWA both contribute to achieving the theoretical  
12 water necessary, improving the internal curing efficiency and preparing non-shrinkage  
13 UHPC.

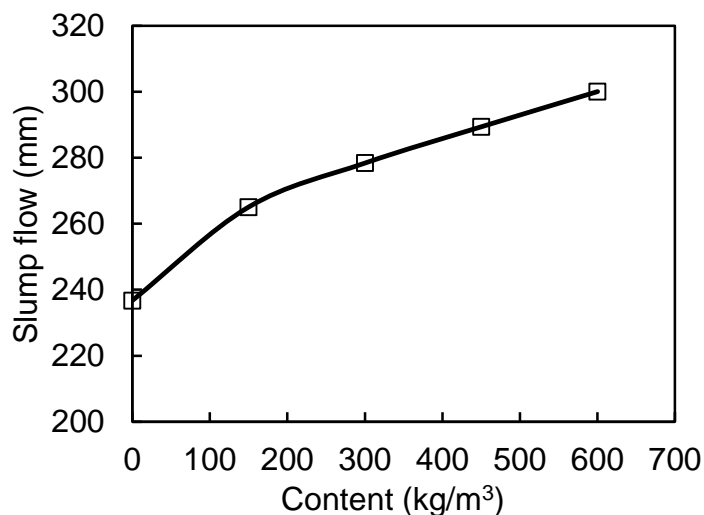


Figure 19 The effect of LWA content on the workability of UHPC



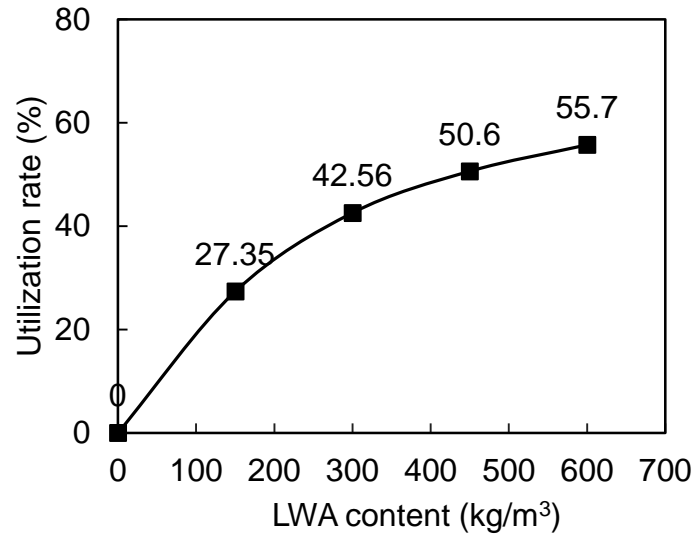


Figure 20 The utilization rate of internal curing water of LWA in UHPC

## 1 **5. Conclusion**

2 A comprehensive investigation of water desorption characteristics of saturated  
3 lightweight fine aggregate in ultra-high performance concrete is presented. The water  
4 desorption characteristics of LWA in UHPC and its effect on the hydration and  
5 microstructure are systemically investigated. Based on this experimental investigation,  
6 the following conclusions can be drawn.

7 (1) The LWA used in this study possesses a large porosity, which can absorb large  
8 amount of free water. Most of the pores are larger than 100 nm, which leads to a rapid  
9 water absorption and easy water desorption at high RH. This indicates that the LWA is  
10 an efficient aggregate which is available for the internal curing of the cementitious  
11 materials.

12 (2) The water desorption of LWA improves the internal RH not only at early age  
13 but also at later age. Some water is released when the UHPC is still in the state of  
14 mixture due to the low internal RH. As a result, although the hydration rate and

---

1 hydration degree of UHPC are both obviously improved, the pore structure is  
2 deteriorated leading to the reduction of compressive strength at early age. However, as  
3 the water desorption proceeds, this adverse effect is overwhelmed by the effect of  
4 internal curing of LWA.

5 (3) Much water desorbs rapidly before setting due to the very low water to binder  
6 ratio. The water also desorbs quickly between 6 h and 24 h, and most of the water has  
7 been already released during the first day. For sample containing  $450\text{kg/m}^3$  of LWA,  
8 there is about 85% of pre-soaked water in LWA which has been released before 40 h,  
9 and at least 49.4% of presoaked water is not for internal curing. The water desorption  
10 of LWA is not only controlled by RH gradient but also other factors such as pore  
11 structure and LWA content.

12 (4) A “four-stage desorption” mechanism driven by capillary pressure and RH  
13 gradient is proposed in the study. This process can be divided into 4 stages: the first and  
14 second stages occur before setting, which is mainly motivated by RH gradient; The  
15 water desorption in the third and fourth stages is used for internal curing. The water  
16 desorption that is beneficial for the internal curing is calculated. It is indicated the  
17 internal curing efficiency could be enhanced by increasing LWA content and reducing  
18 pore size.

19

## 20 **Acknowledgements**

21 This work was financially supported by the National Key R&D Program of China

---

1 (No. 2017YFB0310001) and the National Natural Science Foundation of China (No.  
2 51772226 and U1305245).

3

---

## 1 Reference

- 2 [1] R. Yu, P. Spiesz, H.J.H. Brouwers, Development of an eco-friendly Ultra-High  
3 Performance Concrete (UHPC) with efficient cement and mineral admixtures uses,  
4 Cement and Concrete Composites 55 (2015) 383-394.
- 5 [2] R. Yu, P. Spiesz, H.J.H. Brouwers, Mix design and properties assessment of Ultra-High  
6 Performance Fibre Reinforced Concrete (UHPFRC), Cement and Concrete Research  
7 56 (2014) 29-39.
- 8 [3] P. Shen, L. Lu, Y. He, F. Wang, S. Hu, The effect of curing regimes on the mechanical  
9 properties, nano-mechanical properties and microstructure of ultra-high performance  
10 concrete, Cement and Concrete Research 118 (2019) 1-13.
- 11 [4] M. Cheyrezy, V. Maret, L. Frouin, Microstructural analysis of RPC (Reactive Powder  
12 Concrete), Cement and Concrete Research 25(7) (1995) 1491-1500.
- 13 [5] Y. Bao, W. Meng, Y. Chen, G. Chen, K.H. Khayat, Measuring mortar shrinkage and  
14 cracking by pulse pre-pump Brillouin optical time domain analysis with a single optical  
15 fiber, Materials Letters 145 (2015) 344-346.
- 16 [6] P. Shen, L. Lu, Y. He, M. Rao, Z. Fu, F. Wang, S. Hu, Experimental investigation on  
17 the autogenous shrinkage of steam cured ultra-high performance concrete, Construction  
18 & Building Materials 162 (2018) 512-522.
- 19 [7] D.Y. Yoo, S.W. Kim, Y.S. Yoon, J.J. Park, Benefits of using expansive and shrinkage-  
20 reducing agents in UHPC for volume stability, Magazine of Concrete Research 66(14)  
21 (2015) 745-750.
- 22 [8] K. Koh, G. Ryu, S. Kang, J. Park, S. Kim, Shrinkage properties of ultra-high  
23 performance concrete (UHPC), Advanced Science Letters 4(3) (2011) 948-952.
- 24 [9] V. Corinaldesi, A. Nardinocchi, J. Donnini, The influence of expansive agent on the  
25 performance of fibre reinforced cement-based composites, Construction and Building  
26 Materials 91 (2015) 171-179.
- 27 [10] F. Wang, J. Yang, S. Hu, X. Li, H. Cheng, Influence of superabsorbent polymers on  
28 the surrounding cement paste, Cement and Concrete Research 81 (2016) 112-121.
- 29 [11] P. Lura, M. Wyrzykowski, C. Tang, E. Lehmann, Internal curing with lightweight  
30 aggregate produced from biomass-derived waste, Cement & Concrete Research 59(59)  
31 (2014) 24-33.
- 32 [12] N.V. Tuan, G. Ye, K.V. Breugel, Internal curing of ultra high performance concrete  
33 by using rice husk ash, International Conference on Material Science and Rilem Week,  
34 Rilem, 2010.
- 35 [13] D.P. Bentz, W.J. Weiss, Internal Curing: A 2010 State-of-the-Art Review, NIST  
36 Interagency/Internal Report (NISTIR) - 7765 (2011).
- 37 [14] S. Gaurav, D. Mukul, B. Dale, L. Pietro, C.F. Ferraris, J.W. Bullard, W. Jason,  
38 Detecting the Fluid-to-Solid Transition in Cement Pastes: Comparing experimental and  
39 numerical techniques, Concrete International 36(1) (2009) 53-58.
- 40 [15] P. Lura, J. Couch, O.M. Jensen, J. Weiss, Early-age acoustic emission measurements

- 
- 1 in hydrating cement paste: evidence for cavitation during solidification due to self-  
2 desiccation, *Cement and Concrete Research* 39(10) (2009) 861-867.
- 3 [16] D.P. Bentz, O.M. Jensen, Mitigation strategies for autogenous shrinkage cracking,  
4 *Cement and Concrete Composites* 26(6) (2004) 677-685.
- 5 [17] D.P. Bentz, Influence of internal curing using lightweight aggregates on interfacial  
6 transition zone percolation and chloride ingress in mortars, *Cement & Concrete*  
7 *Composites* 31(5) (2009) 285-289.
- 8 [18] J. Yang, F. Wang, Z. Liu, Y. Liu, S. Hu, Early-state water migration characteristics of  
9 superabsorbent polymers in cement pastes, *Cement and Concrete Research* 118 (2019)  
10 25-37.
- 11 [19] W. Meng, K. Khayat, Effects of saturated lightweight sand content on key  
12 characteristics of ultra-high-performance concrete, *Cement & Concrete Research* 101  
13 (2017) 46-54.
- 14 [20] M. Valipour, K.H. Khayat, Coupled effect of shrinkage-mitigating admixtures and  
15 saturated lightweight sand on shrinkage of UHPC for overlay applications,  
16 *Construction and Building Materials* 184 (2018) 320-329.
- 17 [21] Peiliang Shen , Fazhou Wang, Yongjia He, Shuguang Hu, Internal curing using  
18 lightweight fine aggregate in ultra-high performance concrete, *Cement & Concrete*  
19 *Composites* (2018) submitted.
- 20 [22] K. Janković, S. Stanković, D. Bojović, M. Stojanović, L. Antić, The influence of  
21 nano-silica and barite aggregate on properties of ultra high performance concrete,  
22 *Construction and Building Materials* 126 (2016) 147-156.
- 23 [23] C. Poon, S. Kou, L. Lam, Compressive strength, chloride diffusivity and pore  
24 structure of high performance metakaolin and silica fume concrete, *Construction and*  
25 *Building Materials* 20(10) (2006) 858-865.
- 26 [24] J. Clarke, *Lightweight Aggregate Concrete, Science, technology and Applications,*  
27 *Concrete* (Feb) (2003).
- 28 [25] D.P. Bentz, M.R. Geiker, K.K. Hansen, Shrinkage-reducing admixtures and early-age  
29 desiccation in cement pastes and mortars, *Cement & Concrete Research* 31(7) (2001)  
30 1075-1085.
- 31 [26] BENTUR, Amon, IGARASHI, ShinIchi, KOVLER, Konstantin, Prevention of  
32 autogenous shrinkage in high-strength concrete by internal curing using wet lightweight  
33 aggregates, *Cement & Concrete Research* 31(11) (2001) 1587-1591.
- 34 [27] D. Cusson, T. Hoogeveen, Internal curing of high-performance concrete with pre-  
35 soaked fine lightweight aggregate for prevention of autogenous shrinkage cracking,  
36 *Cement & Concrete Research* 38(6) (2008) 757-765.
- 37 [28] R. Siddique, Compressive strength, water absorption, sorptivity, abrasion resistance  
38 and permeability of self-compacting concrete containing coal bottom ash, *Construction*  
39 *and Building Materials* 47 (2013) 1444-1450.
- 40 [29] J.T. Kevern, Q.C. Nowasell, Internal curing of pervious concrete using lightweight  
41 aggregates, *Construction & Building Materials* 161 (2018) 229-235.

- 
- 1 [30] X. Liu, K.S. Chia, M.H. Zhang, Water absorption, permeability, and resistance to  
2 chloride-ion penetration of lightweight aggregate concrete, *Construction & Building*  
3 *Materials* 25(1) (2011) 335-343.
- 4 [31] L. R., Determining the water absorption of coarse lightweight aggregate for concrete,  
5 Portland Cement Association, Research and Development Laboratories, Skokie, Illinois,  
6 1964.
- 7 [32] A. Radlinska, F. Rajabipour, B. Bucher, R. Henkensiefken, G. Sant, J. Weiss,  
8 Shrinkage Mitigation Strategies in Cementitious Systems: A Closer Look at Differences  
9 in Sealed and Unsealed Behavior, *Transportation Research Record Journal of the*  
10 *Transportation Research Board* 2070(2070) (2008) 59-67.
- 11 [33] P.M. Halleck, D.P. Bentz, Water Movement during Internal Curing: Direct observation  
12 using X-ray microtomography, *Concrete International Design & Construction* 28(10)  
13 (2006) 39-50.
- 14 [34] R. Henkensiefken, T. Nantung, J. Weiss, Saturated Lightweight Aggregate for Internal  
15 Curing in Low w/c Mixtures: Monitoring Water Movement Using X - ray Absorption,  
16 *Strain* 47(s1) (2011) 432-441.
- 17 [35] J. Castro, L. Keiser, M. Goliás, J. Weiss, Absorption and desorption properties of fine  
18 lightweight aggregate for application to internally cured concrete mixtures, *Cement &*  
19 *Concrete Composites* 33(10) (2011) 1001-1008.
- 20 [36] P. Trtik, B. Münch, W.J. Weiss, A. Kaestner, I. Jerjen, L. Josic, E. Lehmann, P. Lura,  
21 Release of internal curing water from lightweight aggregates in cement paste  
22 investigated by neutron and X-ray tomography, *Nuclear Inst & Methods in Physics*  
23 *Research A* 651(1) (2011) 244-249.
- 24 [37] Standard for test methods of long-term performance and durability of ordinary  
25 concrete, Chinese Standard GB/T50082-2009, Beijing 2009.
- 26 [38] Standard test method for chemical shrinkage of hydraulic cement paste., American  
27 Society for Testing and Materials, West Conshohocken, 2007.
- 28 [39] Chinese Standards, Test Method for Fluidity of Cement Mortar, Chinese Standards  
29 Association, China, 2005.
- 30 [40] A. Hajibabae, M.T. Ley, The impact of wet curing on curling in concrete caused by  
31 drying shrinkage, *Materials & Structures* 49(5) (2016) 1629-1639.
- 32 [41] A.C. Kak, M. Slaney, Principles of Computerized Tomographic Imaging, 29(1) (2002)  
33 107-107.
- 34 [42] S. Asamoto, T. Ishida, K. Maekawa, ANALYSIS OF CONCRETE SHRINKAGE  
35 COUPLING WITH PROPERTIES OF AGGREGATE, *Journal of Japan Society of*  
36 *Civil Engineers Ser E1* 63(2) (2007) 327-340.
- 37 [43] D.P. Bentz, K.K. Hansen, H.D. Madsen, F. Vallée, E.J. Griesel, Drying/hydration in  
38 cement pastes during curing, *Materials & Structures* 34(9) (2001) 557-565.
- 39 [44] O.M. Jensen, P.F. Hansen, Water-entrained cement-based materials: II. Experimental  
40 observations, *Cement and Concrete Research* 32(6) (2002) 973-978.
- 41 [45] X. Ma, J. Liu, C. Shi, A review on the use of LWA as an internal curing agent of high

- 
- 1 performance cement-based materials, *Construction and Building Materials* 218 (2019)  
2 385-393.
- 3 [46] S. Nie, S. Hu, F. Wang, P. Yuan, Y. Zhu, J. Ye, Y. Liu, Internal curing – A suitable  
4 method for improving the performance of heat-cured concrete, *Construction &*  
5 *Building Materials* 122 (2016) 294-301.
- 6 [47] T. Powers, Capillary continuity or discontinuity in cement paste, *Pca Bullentin* 110  
7 (1959).
- 8 [48] G. Espinoza-Hijazin, M. Lopez, Extending internal curing to concrete mixtures with  
9 W/C higher than 0.42, *Construction & Building Materials* 25(3) (2011) 1236-1242.
- 10 [49] P.K. Mehta, P.J.M. Monteiro, I. ebrary, *Concrete: microstructure, properties, and*  
11 *materials*, McGraw-Hill New York 2006.
- 12 [50] M.S. Choi, J.S. Lee, K.S. Ryu, K.-T. Koh, S.H. Kwon, Estimation of rheological  
13 properties of UHPC using mini slump test, *Construction and Building Materials* 106  
14 (2016) 632-639.
- 15 [51] A.M. Neville, *Properties of concrete*, 4th and final ed., Wiley, New York, 1996.
- 16 [52] L. Helfen, F. Dehn, P. Mikulík, T. Baumbach, Synchrotron-radiation X-ray  
17 tomography: a method for the 3D verification of cement microstructure and its  
18 evolution during hydration, *Nanotechnology in Construction* (2004), 89-100.
- 19 [53] E. Gallucci, K. Scrivener, A. Groso, M. Stampanoni, G. Margaritondo, 3D  
20 experimental investigation of the microstructure of cement pastes using synchrotron X-  
21 ray microtomography ( $\mu$ CT), *Cement and Concrete Research* 37(3) (2007) 360-368.
- 22 [54] D.P. Bentz, P.M. Halleck, A.S. Grader, J.W. Roberts, Four-dimensional X-ray  
23 microtomography study of water movement during internal curing, *Proceedings of the*  
24 *International RILEM Conference-Volume Changes of Hardening Concrete: Testing and*  
25 *Mitigation*, (2006)11-20.
- 26 [55] O.M. Jensen, P. Lura, K. Kovler, *Volume changes of hardening concrete: testing and*  
27 *mitigation*, RILEM, 2006.

28